

Efficient Evaluation of Energy Focusing Based on Eigen-Beamforming

Thomas Pairon, Claude Oestges, Maxime Drouguet, Christophe Craeye
ICTEAM, Université catholique de Louvain, Louvain-la-Neuve, Belgium, thomas.pairon@uclouvain.be

Abstract—We provide an efficient Method-of-Moments analysis of 2D fields radiated in a typical indoor environment which is applied to the wireless power transfer from a multiple-antenna access point to multiple devices. These simulations allow the computation of the correlation matrix obtained at the access point array when several devices are active. Power focusing capabilities from the same array are then analyzed, including multipath effects. This technique is based on the eigen-analysis of the correlation matrix measured at the access point and presents similarities with time reversal.

Index Terms—antenna arrays, focusing, correlation matrix, time reversal.

I. INTRODUCTION

Focusing of microwave power using antenna arrays is a quite classical subject [1]–[3]. It recently gained momentum with the idea of powering electronic devices in Internet-of-Things applications [4], [5].

A well-known technique for focusing power corresponds to time reversal, which remains effective in rich multipath environments. In a nutshell, a virtual transmitter is placed at the focal point and fields are observed at the level of the different transmitting antennas. The signals from those antennas then corresponds to the complex conjugate of the received field, which in time domain corresponds to a time-reversed signal [6]–[8]. Loosely speaking, the signal propagates back to the transmitter, via all multiples paths. This method has been firstly developed for acoustic problems [6]–[8], before being extended to radio frequencies [9].

However, for narrowband signals, multiple focii are created and a limitation of the resulting spillover requires a proper design of the array configuration. Besides, the estimation of the fields received from the source require a specific attention from the hardware point of view. Indeed, those fields need to be estimated coherently in a noise environment, with one or several (uncorrelated) sources.

The goal of the present paper consists in providing efficient numerical and analytical frameworks for the study of the beamforming weights to be applied to focus the beam in a given direction. Compared to [9], where the environment is modelled with stochastic geometry, this paper treats deterministic site-specific scenarios. The numerical framework corresponds to a 2D Method of Moments, accelerated using multipole decomposition [10], for both the solution of the integral equation and observation of fields. The analytical framework corresponds to an eigenvalue study of the correlation matrix of signals received by one or several sources [11],

where the simulations are carried out with finite difference techniques.

Section II explains the numerical framework as well as the derivation of the beamformer weights. Section III illustrates some results in a complex environment for different bandwidth.

II. EIGEN-BEAMFORMING STRATEGY

A. Acceleration of the full-wave fields computation

The beamforming weights are computed based on the fields radiated by different sources in a complex environment. Different techniques are available for this purpose, such as ray-tracing approaches [12] or physical optics approximation [13]. In this paper, a full-wave solution is provided with the help of the Method of Moments (MoM) which solves the Electric Field Integral Equation (EFIE) and takes into account all the scattering mechanisms (reflection and diffraction).

The major drawback of this method is its complexity which leads to high memory requirements ($\mathcal{O}(N^2)$) and computational time ($\mathcal{O}(N^3)$); however, it provides an exact solution of the Maxwell's equations, barring the discretization error. It is then more accurate than physical optics (PO) which fails to predict precisely the fields away from the specular direction, while providing a $\mathcal{O}(N)$ memory complexity. Ray-tracing techniques allow the fast evaluation of the scattered field by flat surfaces at high frequencies. While providing a reduced computational time, this technique is not well suited for complex geometries.

MoM consists in computing the equivalent currents induced by an incident field on the scatterers' surface. The fields radiated by those currents added to the incident field provide the total field distribution over the considered area. Those currents \mathbf{I} are the solution of the linear system :

$$\mathbf{Z}\mathbf{I} = -\mathbf{v}, \quad (1)$$

where \mathbf{v} is the incident field on the scatterers' surface and \mathbf{Z} is the impedance matrix. With the surfaces discretized with N basis functions, \mathbf{Z} is a dense square matrix of size $(N \times N)$ whose elements are expressed as [14] :

$$Z_{i,j} \simeq \int_i \mathbf{f}_i \int_j \mathbf{f}_j G(k|\vec{r}_{i,j}|) dC_j dC_i, \quad (2)$$

where \mathbf{f} are the basis functions, k is the wave number, $G(x) = -j/4H_0^2(x)$ is the 2D Green's function for the

Helmholtz' equation, $j = \sqrt{-1}$, $|\vec{r}_{i,j}|$ is the distance between two basis functions and $i, j \in [1 \dots N]$.

In order to accelerate the filling of \mathbf{Z} , the domain is decomposed in M groups of N' basis functions. The basic idea of the fast multipole method (FMM) is to compute the interactions of the basis functions with its center (*aggregation* step), translate the fields to the center of the testing group (*translation* step) and finally transmit those fields to the testing functions (*disaggregation* step). The filling time of (2) is performed through the Green's function decomposition written as [15] :

$$H_0^2(k\vec{r}_{i,j}) = \frac{1}{2\pi} \int_0^{2\pi} P_{j,n}(\alpha) T_{m,n}(\alpha) P'_{m,i}(\alpha) d\alpha, \quad (3)$$

with

$$\begin{aligned} P_{j,n}(\alpha) &= \exp(-jk|\vec{r}_{j,n}|\cos(\alpha - \phi_{j,n})), \\ T_{m,n}(\alpha) &= \sum_{p=-P}^P H_p^2(k|\vec{r}_{m,n}|) \exp(-jp(\phi_{m,n} - \alpha + \pi/2)), \\ P_{m,i}(\alpha) &= \exp(jk|\vec{r}_{i,m}|\cos(\alpha - \phi_{i,m})), \end{aligned}$$

where m, n refer to the groups containing i, j basis functions and ϕ is the angle between a basis function and the center of its group ($\phi_{i/j,m/n}$) or the angle between the center of two groups ($\phi_{m,n}$). An important observation is that $T_{m,n}$ only depends on the distance between the groups. That means that any interaction between basis and testing functions of the groups m and n is expressed with the same transfer function. If M and N' are chosen so that $N = M = N'$, the number of operations required to fill \mathbf{Z} shrinks from N^2 to $N^{1.5}$.

B. Computation of the steering vectors

The computation of the weights required to steer the beam towards N_d different devices is performed using the correlation matrix available at the access point. Let \mathbf{y} of size $N_a \times 1$ be the signals at each of the N_a -antenna access point, with $N_d < N_a$. The correlation matrix \mathbf{C} of size $N_a \times N_a$ is defined as :

$$\mathbf{C} = \mathbb{E}(\mathbf{y}\mathbf{y}^H). \quad (4)$$

By ergodicity, the expectation is computed as the average over the sampled signals at different time instants. The matrix \mathbf{C} is then factorized using the eigenvalue decomposition (EVD) as follows :

$$\mathbf{C} = \mathbf{U}_C \mathbf{\Lambda}_C \mathbf{U}_C^H, \quad (5)$$

where the subscript C refers to the correlation matrix and superscript H is the hermitian operator. The weights of the beamformer corresponding to the N_d devices are selected as the complex conjugate of the N_d vectors of \mathbf{U}_C associated to the N_d non-zero eigenvalues of $\mathbf{\Lambda}_C$. Working with the correlation matrix, as already done for localization [16], rather than instantaneous snapshots avoids potential problems with residual Doppler cancellation and enables efficient noise suppression using time averaging.

Note that under the assumption of uncorrelated sources, eigenvectors of the correlation matrix are exactly equal to the

left singular vectors of the channel matrix \mathbf{H} of size $N_a \times N_d$, defined as :

$$\mathbf{y} = \mathbf{H}\mathbf{x}, \quad (6)$$

where \mathbf{x} of size $N_d \times 1$ represents the uncorrelated signals transmitted by each device. Inserting (6) in (4), under the assumption that \mathbf{H} is constant, one can derive :

$$\mathbf{C} = \mathbb{E}(\mathbf{H}\mathbf{x}\mathbf{x}^H\mathbf{H}^H) = \mathbf{H}\mathbb{E}(\mathbf{x}\mathbf{x}^H)\mathbf{H}^H. \quad (7)$$

If vectors \mathbf{x} are uncorrelated over time and the various devices, $\mathbb{E}(\mathbf{x}\mathbf{x}^H)$ is the identity matrix. Under those assumptions, one can write

$$\mathbb{E}(\mathbf{y}\mathbf{y}^H) = \mathbf{H}\mathbf{H}^H. \quad (8)$$

Using the singular value decomposition (SVD) of $\mathbf{H} = \mathbf{U}_H \mathbf{\Sigma}_H \mathbf{V}_H^H$, we find that $\mathbf{C} = \mathbf{U}_H \mathbf{\Sigma}_H^2 \mathbf{U}_H^H$. Using (5), we find that :

$$\begin{aligned} \mathbf{U}_C &= \mathbf{U}_H, \\ \mathbf{\Lambda}_C &= \mathbf{\Sigma}_H^2. \end{aligned}$$

It has been shown that the weights are equally obtained using EVD on the correlation matrix \mathbf{C} or SVD on the channel matrix \mathbf{H} . Nevertheless, the knowledge of \mathbf{H} is not always available in practice and requires to send pilots which increases the system complexity.

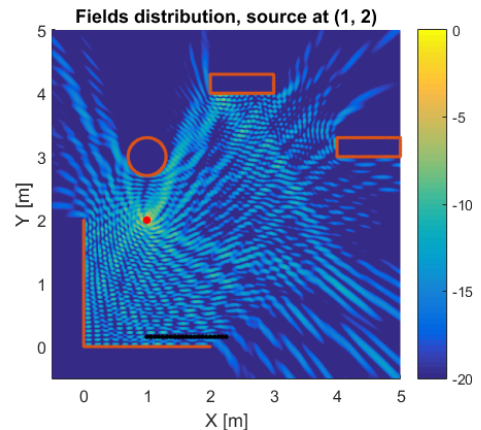
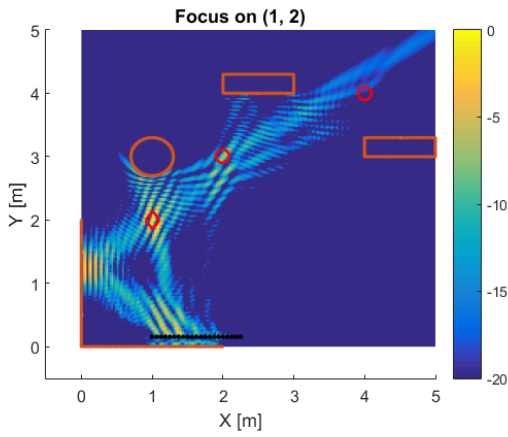


Fig. 1: Fields distribution with multiple reflections. The line source is located at (1, 2). The orange lines represent the obstacles, the black dots are the elements of the access point array, the red dot is the line source. The working frequency is 2.4 GHz.

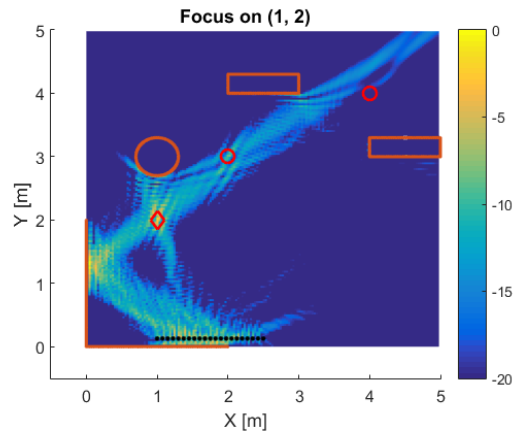
III. NUMERICAL RESULTS

A. Field distribution

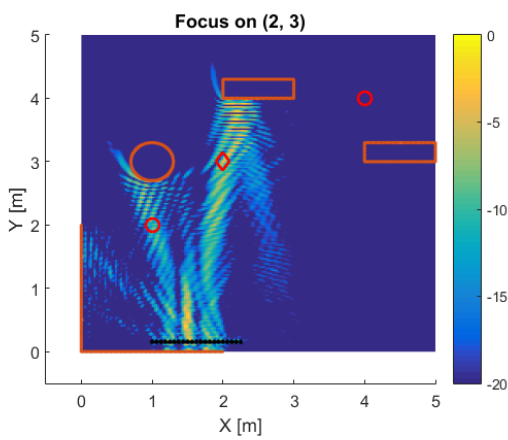
Simulations have been carried out in a 2D configuration, where walls and furniture are represented as conducting strips or cylinders with rectangular cross-sections made of perfectly electric conductors (PEC). The proposed method can be extended to dielectric objects with the PMCHWT formulation [17]. This extension is not considered in this paper. The devices on which the energy is focused consist of a collection



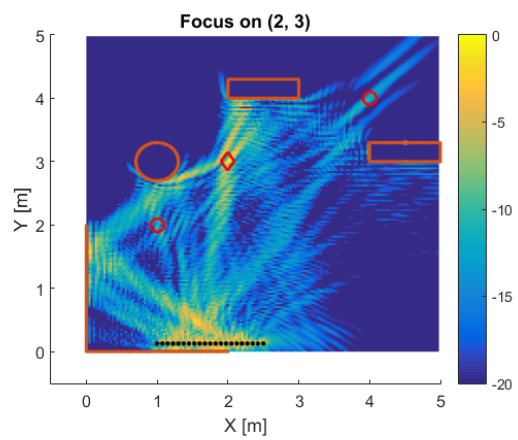
(a) Power steered at device1, located at (1, 2).



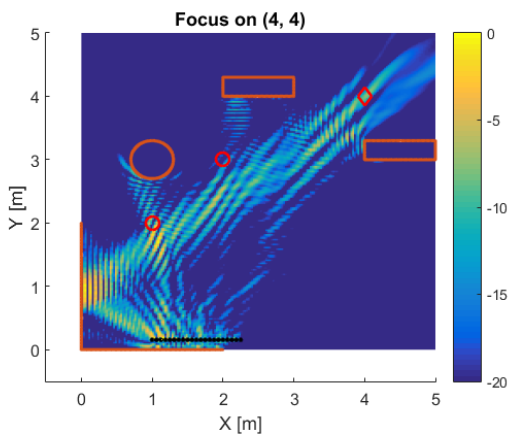
(a) Power steered at device1, located at (1, 2).



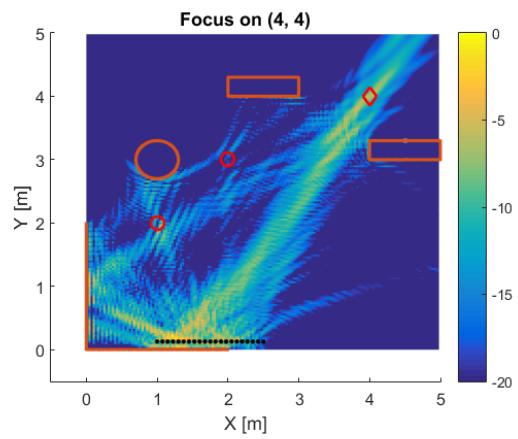
(b) Power steered at device2, located at (2, 3).



(b) Power steered at device2, located at (2, 3).



(c) Power steered at device3, located at (4, 4).



(c) Power steered at device3, located at (4, 4).

Fig. 2: Beam steered in the 3 different directions. Signal bandwidth is $[2.5\text{GHz} \pm 50 \text{ MHz}]$. Orange lines represent the reflectors, black dots the transmitting array, red circles are the positions of the devices. For each figure, red diamond represents the selected device.

Fig. 3: Beam steered in the 3 different directions. Signal bandwidth is $[2.5\text{GHz} \pm 500 \text{ MHz}]$. Orange lines represent the reflectors, black dots the transmitting array, red circles are the positions of the devices. For each figure, red diamond represents the selected device.

of line sources. In the transmitting configuration, each line source is excited consecutively and induced currents are computed on the surfaces. Those currents are computed using the Method of Moments (MoM), considering a TM polarisation. This procedure is accelerated through the FMM algorithm presented in Section II. Likewise, in the receiving case, the signals originating from several sources and impinging on the different elements of the array can be computed.

One can observe on Fig. 1 that, even with a limited number of obstacles, the field distribution is characterized by a rich multipath signature. This may actually be favorable to focusing, since power can reach the device to be fed after reflection or diffraction on walls and furniture.

B. Energy focusing on different sources

The access point linear array comprises 21 antennas with a $\lambda/2$ space between adjacent elements. The signals transmitted by the three devices are added coherently at the access point and are uncorrelated. The system is assumed without noise ($\text{SNR} = \infty$).

From there, the transfer matrix \mathbf{H} is computed for all pairs of devices and access point antennas. A singular value decomposition of this matrix is then performed and singular vectors associated to dominant single values are used for focusing. The weights used for beamforming simply correspond to the conjugate of the dominant eigenvectors. We emphasise that in a practical implementation, with no knowledge of the channel matrix, the weights are computed based on the correlation matrix. Both methods are equivalent under the assumptions detailed in Section II-B.

A bandwidth for the two signals of 100 MHz (Fig. 2) and 1 GHz (Fig. 3) are here considered, using 11 equally spaced tones in the band. The total field average power is then computed using Parseval's theorem as :

$$P_t(x, y) = \int |\mathbf{E}_t(x, y, \omega)|^2 d\omega \quad (9)$$

It is observed that effective focusing is achieved onto both sources and that reflection on walls is efficiently exploited. This is clearly visible on Fig. 3a and Fig. 3b, where the signal is reflected on the wall. Larger bandwidth tends to reduce the sidelobes around the focal point, as depicted on Fig. 2. Note that the size of the main beam does not depend on the bandwidth of the signal but is related to the scattering richness [9]. This is observable when comparing Fig. 3b and Fig. 3c. For the former, the total field is a combination of direct path, strong reflections and diffraction on the cylinder; for the latter, the direct path is dominant, which leads to a larger main beam.

IV. CONCLUSION

A numerical framework has been developed to evaluate focusing of wireless devices using transmit-receive arrays, considering an eigen-analysis of the correlation matrix measured at the access point. Comparison with the channel matrix has been presented and is mathematically identical when the sources are uncorrelated. The scattered fields are computed

with the Method of Moments, a full-wave solver providing an accurate solution of Maxwell's equations. The complexity of this method has been reduced thanks to the multipole expansion of the Green's function. This approach reduces significantly the computational complexity of the problem.

The proposed framework allows the study of large environments as well as a fine visualisation of the fields. It has been clearly observed that power can be conveyed via walls and other obstacles in a rich multipath environment. The richness of the scattering environment allows a better focalisation of the energy, while the number of antennas and the bandwidth of the signal will impact the amplitude of the sidelobes.

The results presented in this paper are limited to 2D scenarios. The method can be extended to 3D scenarios through a multilevel decomposition of the domain. Problems discretized by hundreds of millions of unknowns are then solved in hours [18]. The higher complexity of 3D problems can be overcome through cluster computing or GPU programming since MoM can be highly parallelized. Until now, the scatterers are considered as PEC. The proposed method can be extended to dielectric objects with a combination of the EFIE and the Magnetic Field Integral Equation (MFIE).

ACKNOWLEDGMENTS

The authors are grateful to Dr. Ivan Stupia from UCLouvain for discussions on power focusing. This work has been partially funded by INNOVIRIS, Région Bruxelloise, through the COPINE project and through a FNRS/FRIA grant from Communauté Française de Belgique.

REFERENCES

- [1] A. Buffi, A. A. Serra, P. Nepa, H. T. Chou, and G. Manara, "A focused planar microstrip array for 2.4 GHz RFID readers," in *IEEE Trans. Antennas Propag.*, vol. 58, pp. 1536-44, 2010.
- [2] Y. Li and V. Jandhyala, "Design of retrodirective antenna arrays for short-range wireless power transmission," in *IEEE Trans. Antennas Propag.*, Vol. 60, pp. 206-211, Jan. 2012.
- [3] M. Ettorre, W.A. Alomar, and A. Grbic, "2-D Van Atta array of wideband, wideangle slots for radiative wireless power transfer systems," in *IEEE Trans. Antennas Propag.*, Vol. 58, pp. 4577-4585, Sep. 2018.
- [4] I. Krikidis, S. Timotheou, S. Nikolaou, G. Zheng, D.W. Kwan Ng, and R. Schober, "Simultaneous wireless information and power transfer in modern communication systems," in *IEEE Commun. Mag.*, Vol. 52, pp. 104-110, Nov. 2014.
- [5] P. Kamalinejad, *et al.*, "Wireless energy harvesting for the Internet of Things," in *IEEE Commun. Mag.*, vol. 53, no. 6, pp. 102-108, June 2015.
- [6] M. Fink and C. Prada, "Ultrasonic focusing with time reversal mirrors," in *Advances in Acoustic Microscopy Series*, (ed.) A. Briggs and W. Arnold, Springer, 1996.
- [7] G. Lerosey, J. De Rosny, A. Tourin, A. Derode, G. Montaldo, M. Fink, "Time reversal of electromagnetic waves," in *Phys. Rev. Lett.*, vol. 92, iss. 19, p. 193904, 2004.
- [8] C. Prada, E. Kerbrat, D. Cassereau, M. Fink, "Time reversal techniques in ultrasonic nondestructive testing of scattering media," in *Inverse Probl.*, Vol. 18, pp. 1761-1773, 2002.
- [9] C. Oestges, *et al.*, "Characterization of space-time focusing in time-reversed random fields," in *IEEE Trans. Antennas Propag.*, vol.53, no. 1, pp. 283-293, 2005.
- [10] R. Coifman, V. Rokhlin and S. Wandzura, "The fast multipole method for the wave equation: A pedestrian prescription," in *IEEE Antennas Propag. Mag.*, Vol. 35, pp. 712, 1993.

- [11] H-H. Kim, H-J. Kim, S.-J. Song, K-C Kim, Y-B Kim, "Simulation based investigation of focusing phased array ultrasound in dissimilar metal welds, in *Nuclear Eng. Techn.*, Vol. 48, pp. 228-235, Jan. 2016.
- [12] S. Grubisic and W. P. Carpes, "An efficient indoor ray-tracing propagation model with a quasi-3D approach," in *J. Microw. Optoelectron. Electromagn. Appl.*, Vol.13, no. 2, pp. 166-176, 2014.
- [13] I. De Coster, *et al.*, "A PO approach for a more accurate calculation of the reflected field in indoor propagation," in *48th IEEE Veh. Technol. Conf.*, Ottawa, Ont., pp. 669-672, 1998.
- [14] W. C. Gibson, "Two-dimensional problems," in *The method of moments in electromagnetics*, Chapman & Hall/CRC, pp. 100-102, 2008.
- [15] W. C. Chew, J. Jin, E. Michielssen and J. Song, "Fast multipole method and multilevel multipole algorithm in 2D," in *Fast and efficient algorithms in computational electromagnetics*, Artech House, Norwood, pp. 39-52, 2001.
- [16] R. Schmidt, "Multiple emitter location and signal parameter estimation, in *IEEE Trans. Antennas Propag.*, Vol. 34, pp. 276-280, 1986.
- [17] K. Umashankar, A. Taflove and S. M. Rao, "Electromagnetic scattering by arbitrary shaped three-dimensional homogeneous lossy dielectric objects," in *IEEE Trans. Ant. Prop.*, vol. 34, no. 6, pp. 758-766, 1986.
- [18] O. Ergil and L. Grel, "Accurate solutions of extremely large integral-equation problems in computational electromagnetics," in *Proc. IEEE.*, vol. 101, no. 2, 2013.